

Porosity Modeling Using Acoustic Impedance and Well Log Data in EK Field, Niger Delta

Ekone N.O^{*}, Ehirim C. N.^{**}, Nwosu J.I.^{**} and Dagogo, T.^{**}

^{*}(World Bank Africa Centre of Excellence, University Of Port Harcourt, Port Harcourt).

Email ask4ekone@gmail.com^{**} (Department of Physics/Geology University of Port Harcourt, Nigeria.)

Abstract:

The purpose of reservoir characterization is to build a detailed geologic model description of the reservoir that gives a good prediction of its future behavior and ensures an optimized production. The primary objective of this study involves the prediction of porosity in the EK oil field of the Niger Delta. The post-stack inversion for direct prediction of porosity was performed by transformation of acoustic impedance and utilizing an estimated porosity log. The 3-D seismic data was used to interpret the location of major structures and stratigraphic markers between wells. An excellent correlation coefficient (0.71) exists between log porosity and acoustic impedance in crossplot model of the study area. The study evaluates a model of porosity characterized by wells and seismic data using seismic inversion and geostatistical methodology. The approach provides a geologically realistic porosity distribution and helps in understanding the reservoir image. The porosity predicted has a good match with the actual average log data of EK wells. The results show the advantages in using the seismic acoustic impedance inversion in the determination of petrophysical properties in Niger delta reservoirs and consequently, more accurate model can be generated and forecasts about the behaviour of a field.

I. INTRODUCTION

Porosity is one of the most significant rock properties in describing porous or permeable media. It is defined as the proportion of pore volume to bulk volume of a rock sample. The most significant utilization of the porosity is to quantify the storage capacity of the reservoir, and, from this gauge the measure of hydrocarbon present can be produced. To effectively estimate the lateral and vertical distribution of porosity in the reservoir, a Stochastic 3D property modeling technique is utilized. Gaussian Simulation covers many related methodologies for estimating reservoir properties away from known points. Sequential Gaussian Simulation, is usually utilized for modeling continuous petrophysical properties. This technique was chosen since it calculates a value property distribution of the input data and they honor the input distribution data more realistically. The main disadvantage identified with this techniques is that far away from the known data, the method generates unrealistic results. One approach to beat this drawback in this modeling method, is by utilizing a second property as a trend. The porosity model in this situation will be guided by a second property that is related to it such like acoustic impedance. Various scientists have demonstrated that a direct relationship exist between acoustic impedance and porosity ([1], [2]). According to the authors [3] acoustic impedance values determined from the 3D seismic inversion data set can be utilized to find the zones of low and high porosities in sandstone reservoirs. Cross plot provides evidence of linear relationship between the acoustic impedance and the porosity present in the log. The zones corresponding with higher porosity values within the reservoir correspond to low impedance values. Geostatistical techniques, such as cokriging, can integrate well-log data and seismic data to improve the lateral resolution of the final results. Cokriging is multivariable estimation method that utilizes the relationship between properties that are related [4]. The goal of the cokriging method is to use attributes, such as acoustic impedance, amplitude or travel time extracted from 3D seismic data, as a secondary variable to guide the interpolation of related primary variable, such as porosity, shale volume or depth of well log data.

In this paper, an attempt is made to integrate wire line logs and seismic data volumes to directly predict the porosity of pay zones in the study area. The study area is located in the swamp region of eastern part onshore, Niger Delta. (Figures 1).

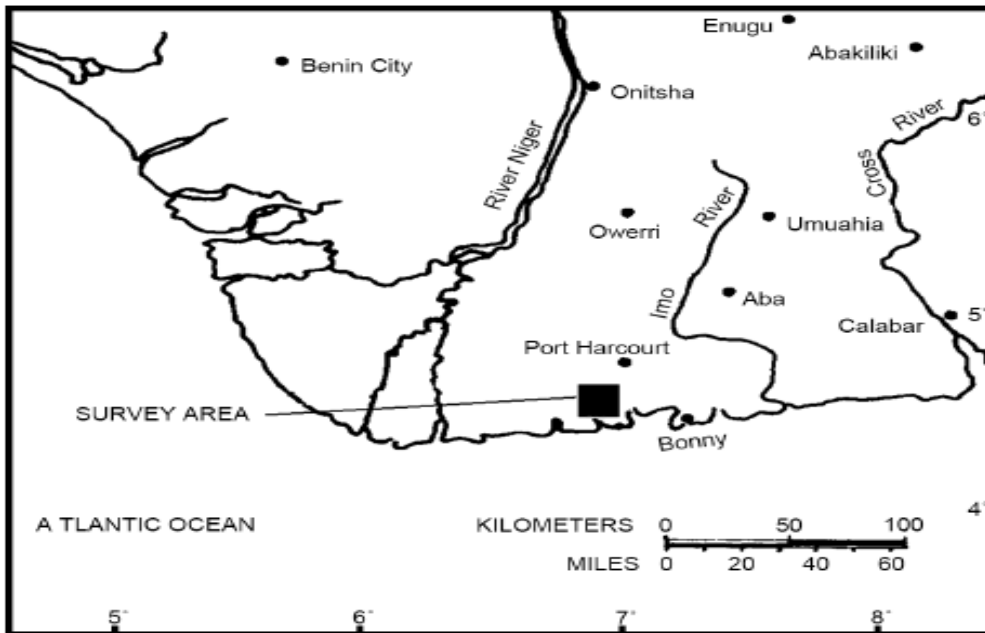


Figure 1: The Location of the study area in the Niger Delta region [5]

II. GEOLOGY OF NIGER DELTA

The Niger Delta is the youngest sedimentary basin within southern Nigeria and the Gulf of Guinea offshore Nigeria. It deltaic and shallow marine sediments began after the Eocene tectonic phase. These deposits have been divided into three broad lithostratigraphic units: (1) the Akata Formation which is the basal Paleocene to Recent pro-delta shale deposits (2) Agbada Formation of Eocene to Recent paralic sequence of sand/shale that overlain the Akata Formation. The Akata Formation is the source rock in the sedimentary basin and the Agbada formation contains most of the reservoir (3) the Benin Formation of Oligocene-Recent fluvial facies of the Niger delta is topmost unit that made up mainly continental upper deltaic plain sands ([6], [7], [8]). Virtually all the hydrocarbon accumulations in the Niger Delta occur in the sands and sandstones of Agbada Formation where they are trapped by rollover anticlines related to growth fault development.

III. MATERIALS AND METHODS

The data set utilized in this work includes a 3D Post Stack Time Migrated (PSTM) Seismic volume (SEG-Y), composite well Logs (ASCII), these logs incorporate Gamma ray (GR), resistivity (LLD) and density (RHOB), sonic log and check shot data. All the data files are in standard digital format. Petrel (A Schlumberger software) was used for the interpretation. This study makes use of model based inversion techniques in the workflow (Figure 2). The well log data were extensively visualized and the gamma ray log used in establishing the shale and clean sand base lines hence used in predicting lithology. Both the gamma ray log and deep resistivity log were used for lithostratigraphic correlation panels of the wells (Figure 3). Petrophysical analysis was done using the petrophysical model equations;

Estimation of Volume of Shale

The Volume of Shale (V_{SHALE}) was estimated using

$$V_{SHALE} = \frac{83}{1000} * \left[2^{\left(\frac{37}{10}\right) * IGR} - 1 \right] \quad [9] \dots \dots \dots (1)$$

Where: IGR is the gamma ray index calculated as;

$$IGR = \frac{(G_{LOG} - G_{MN})}{(G_{MX} - G_{MN})} \quad [10] \dots \dots \dots (2)$$

G_{LOG} = Gamma Ray Log reading of the formation
 G_{MN} = Minimum Gamma Ray for a complete sand (100% clean sand) matrix zone
 G_{MX} = Maximum Gamma Ray for a complete shale zone (100% shale)

Estimation of Porosity

The density log was used to estimate the total porosity (ϕ_{TOTAL}) by Equation (3):

$$\phi_{TOTAL} = \frac{(\rho_{MAT} - \rho_{BULK})}{(\rho_{MAT} - \rho_{FLUID})} \quad ([11], [12]) \dots \dots \dots (3)$$

Where

- ϕ_{TOTAL} = total porosity from density log.
- ρ_{MAT} = matrix density
- ρ_{BULK} = formation bulk density and ρ_{FLUID} = fluid density.

Effective porosity ϕ_{EFF} was estimated using $\phi_{EFF} = (1 - V_{SHALE}) * \phi_{TOTAL} \dots \dots \dots (4)$

Estimation of water saturation

The Archie Equation is utilized in the computation of water saturation. As indicated by author [13], determination of the water saturation for the uninvaded zone is accomplished using the equation (5):

$$S_w^n = (F * R_w) / R_t \dots \dots \dots (5)$$

Where,

- R_t = true formation resistivity (Deep Resistivity)
- R_w = formation water resistivity at formation temperature
- n = Saturation exponent
- F = formation factor

The formation factor is actualize by utilizing the Humble equation:

$$F = a / \phi_{EFF}^m$$

Where,

- F = formation factor
- a = Archie's exponent or tortuosity factor
- ϕ_{EFF} = effective porosity
- m = cementation exponent factor = 2

Thus

$$S_W = \left[\frac{a * R_w}{\phi_{EFF}^m * R_t} \right]^{\frac{1}{n}} \dots \dots \dots (6)$$

A synthetic seismogram was generated from well EK 2 that has checkshot data and this was utilized to tie seismic to well data (Figure 4). In generating synthetic seismogram, sonic log was calibrated with checkshot and used alongside density log to generate acoustic impedance log. The generated acoustic impedance log was however used to generate reflection coefficient series log (RC). This RC log was convolved with a wavelet to generate the synthetic seismogram. Tying well log to seismic data is done by converting well data from depth domain into time domain by checkshot data. The Model-based Inversion was performed using the Petrel software, which is a software widely used in the industry implemented to perform seismic reservoir characterization. The well data has a higher resolution compared with the seismic data and applying a low pass filter, permitting a maximum frequency between 0 Hz and 9 Hz, generating then a low frequency mode which is used in the seismic inversion. A wavelet is then estimated and the inversion performed.

The Cross-plot investigation was used to determine the correlation between primary (porosity) and secondary (impedance) variables. The Standardized conventional cokriging of acoustic impedance well logs was utilized in this work.

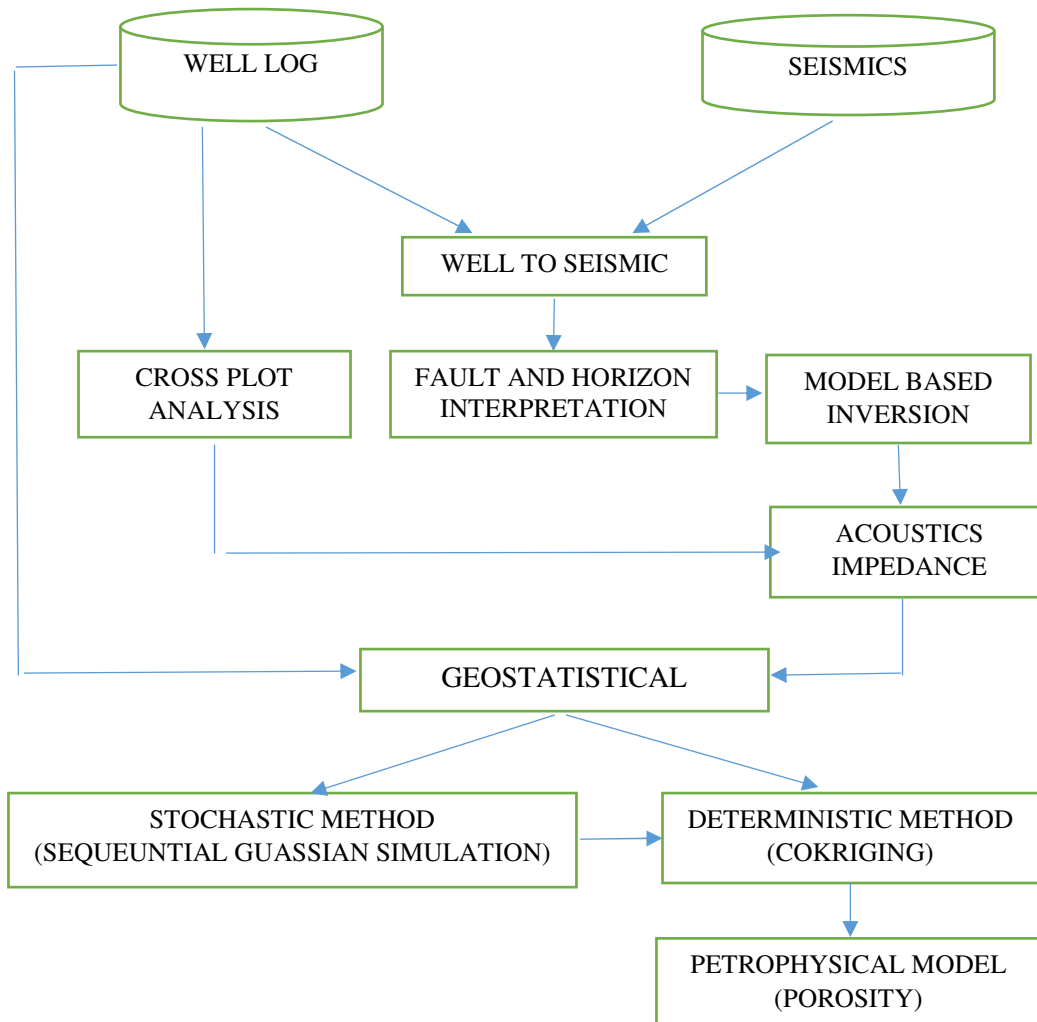


Figure 2: Work flow methodology

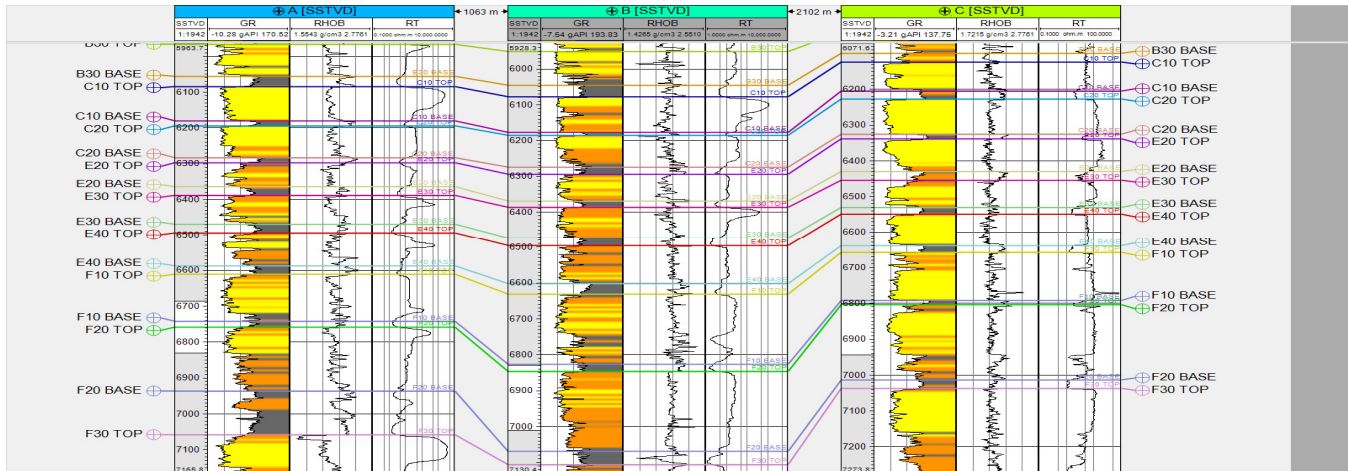


Figure 3: Well Correlation (Sand B30 to F20)

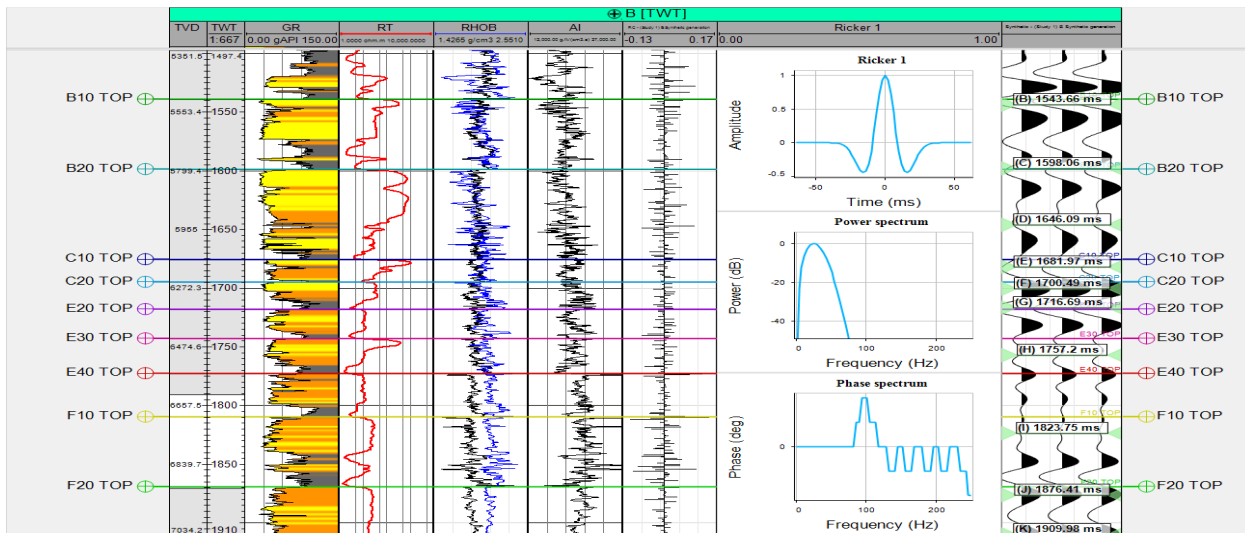


Figure 4: Well-to-Seismic Tie

GEOSTATISTICAL METHODOLOGY

Sequential Gaussian Simulation

The Gaussian Simulation covers many related methodologies for estimating reservoir properties away from known points. The stochastic simulation technique provides a series of equally valid and possible realizations that by implication mirror the distribution of reservoir properties. Each realization was built by the mean and covariance estimated at each grid cell using cokriging.

Cokriging

The cokriging function is a linear blend of primary and secondary variables as show in the equations below.

$$\alpha_0 = \sum_{i=1}^N \alpha_i P_i + \sum_{j=1}^M \beta_j S_j \dots \dots \dots (1)$$

Where α_0 is the estimate at area 0. P_i the primary factor and the number of the primary factors at close by areas is N where $i = 1, \dots, N$. S_j the secondary factor and the number of the secondary factors at close by areas M where $j = 1, \dots, M$. α_i and β_j are the corresponding weights of primary and secondary factors.

For standardized conventional Cokriging, we re-adjust the secondary factor to such an extent the mean of secondary factor can be dealt with as equivalent to the mean of primary factor. The function of standardized conventional Cokriging can be written as

$$\alpha_0 = \sum_{i=1}^N \alpha_i P_i + \sum_{j=1}^M \beta_j (S_j - X_p + X_s) \dots \dots \dots (2)$$

$$\sum_{i=1}^N \alpha_i + \sum_{j=1}^M \beta_j = 1 \dots \dots \dots (4)$$

Where X_p the estimated mean of the primary factor and X_s is the estimated mean of the secondary factor.

IV. PRESENTATION OF RESULT

The results of this study are presented under following headings: petrophysical analysis, structural interpretation, cross plot analysis, inversion result and property modelling.

Petrophysical analysis

Petrophysical parameters were quantitatively estimated using established empirical models for the target reservoir C10. Table 1 shows the results of average calculated petrophysical parameters (total porosity, effective porosity, shale volume and water saturation) for the reservoir zone. The total porosity is 25.98%, 31.35% and 28.85% while effective porosity are 24.41% , 32.10% and 27.77% for well EK1, EK2 and EK3, respectively. Meanwhile, the average water saturation values are 33.43%, 23.29% and 29.12% indicating 66.57%, 76.71% and 70.88% of hydrocarbon saturation respectively. The sands are well sorted with low values of the V_{shale} with an average value of 3.97% - 14.33% for sand C10.

Table 1: Estimated average petrophysical parameters for sand C10

Wells	Depth (ft)	Thickness(ft)	POROT (%)	VSH (%)	POROE (%)	Sw (%)
Wells EK1 C10 Top-C10 Base	6252-6341	89	25.9866	6.6731	24.4159	33.4321
Well EK2 C10 Top- C10 Base	6246-6335	89	31.348	14.3314	32.1031	23.2922
Well EK3 C10 Top-C10 Base	6302-6401	99	28.8531	3.9691	27.7718	29.1231

Structural Interpretation

Fault polygons were generated from faults mapped on the seismic section. Horizons B20, B30 and C10 were mapped with reservoir tops serving as control. The interpreted faults were modeled and pillar gridded which was used to generate 3D grids for the horizons (Figure 5).

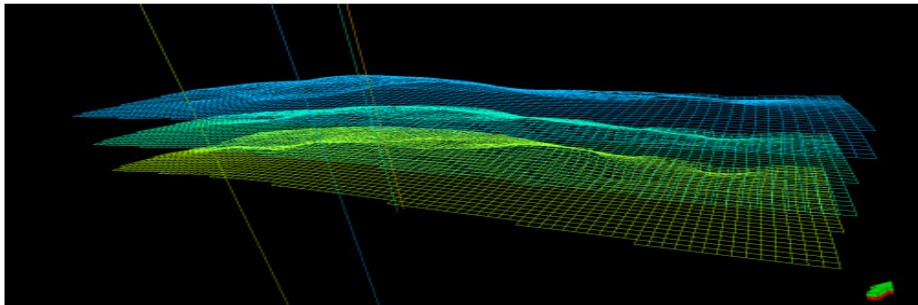


Figure 5. 3D Grid and Wells

Figure 6 and 7 depict the time and depth structural map of the horizon C10. The field structure is a rollover anticline, it is bounded to the north by major synthetic growth faults that characterizes the field. Well EK-2 is located close to the crest of the anticlinal structure and bounded by two major fault structure. These fault may act as sealing fault to this hydrocarbon bearing structure.

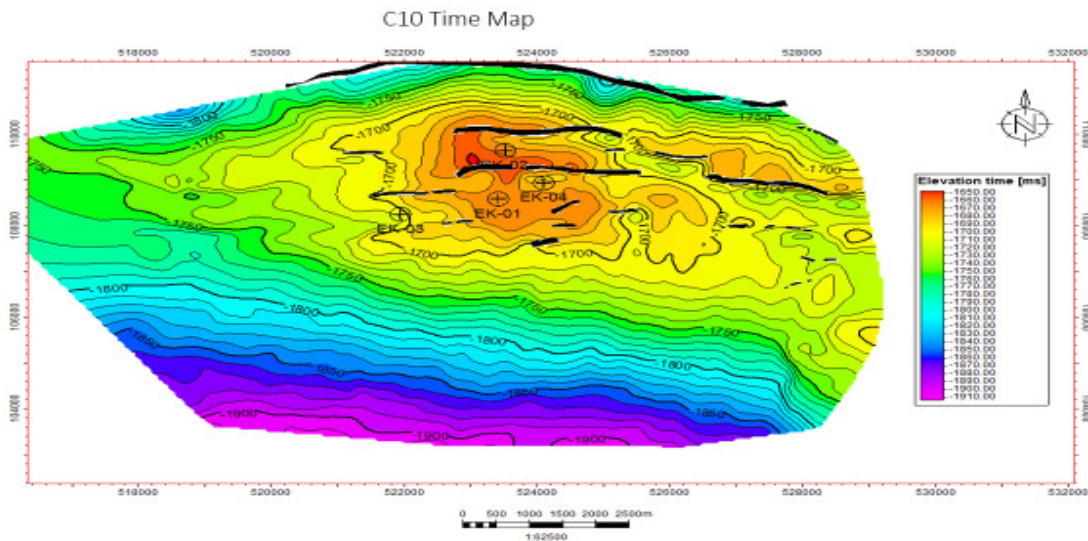


Figure 6 :Time structural map of the horizon C10

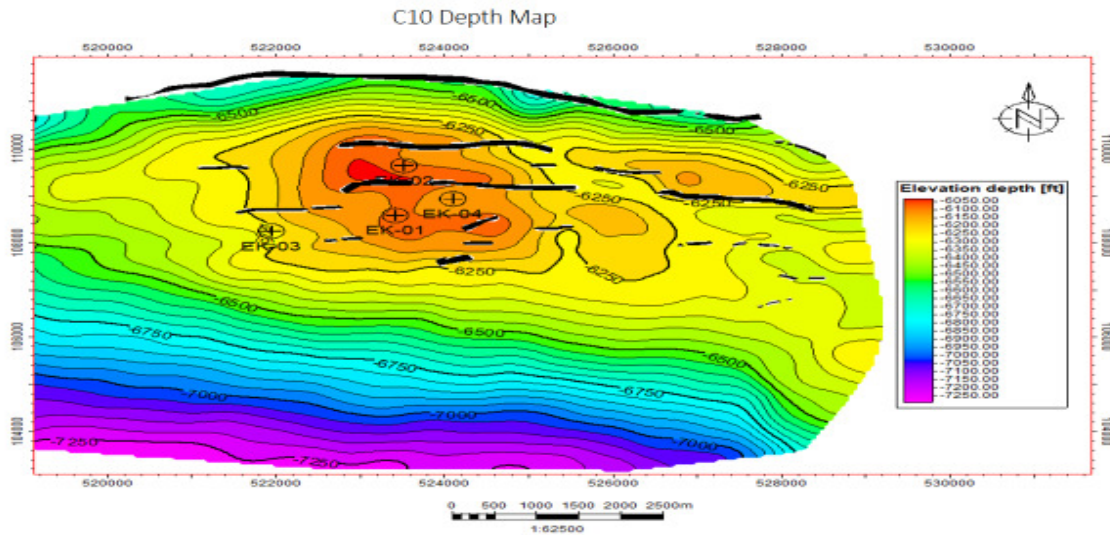


Figure 7 : Depth structural map of the horizon C10.

Cross Plot Analysis

The cross plot of Acoustic impedance against porosity of reservoir C10 shows an inverse relationship between porosity and acoustic impedance (Figure 8a). All clean sand points fit a straight line, and this relationship appears robust and present in all wells. The correlation coefficients of the cross plot has high correlation (0.71) which shows good established correlation between acoustic impedance and reservoir facies (as well as porosity). The cross plot model of Mu-rho versus porosity colour coded with volume of shale for reservoir C10 is shown in Figure 8b. This is an important cross plot that differentiated shale from sand and good litho-fluid discriminator in this reservoir. It shows the separation of hydrocarbon sands (red ellipse) with high Mu-rho from shaly lithology (red ellipse) with low Mu-rho values. Low Mu-rho correspond to high shale volume and low porosity. The hydrocarbon sand indicate high porosity and associated low volume shale (3-13%).

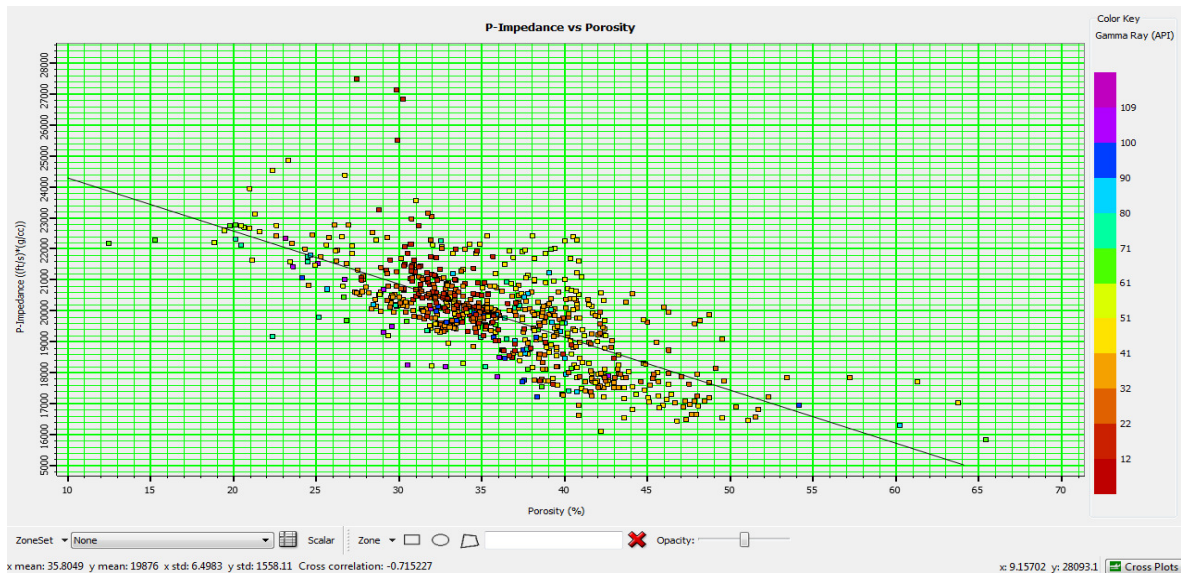


Figure 8: Cross-plot between porosity and acoustic impedance Reservoir C10

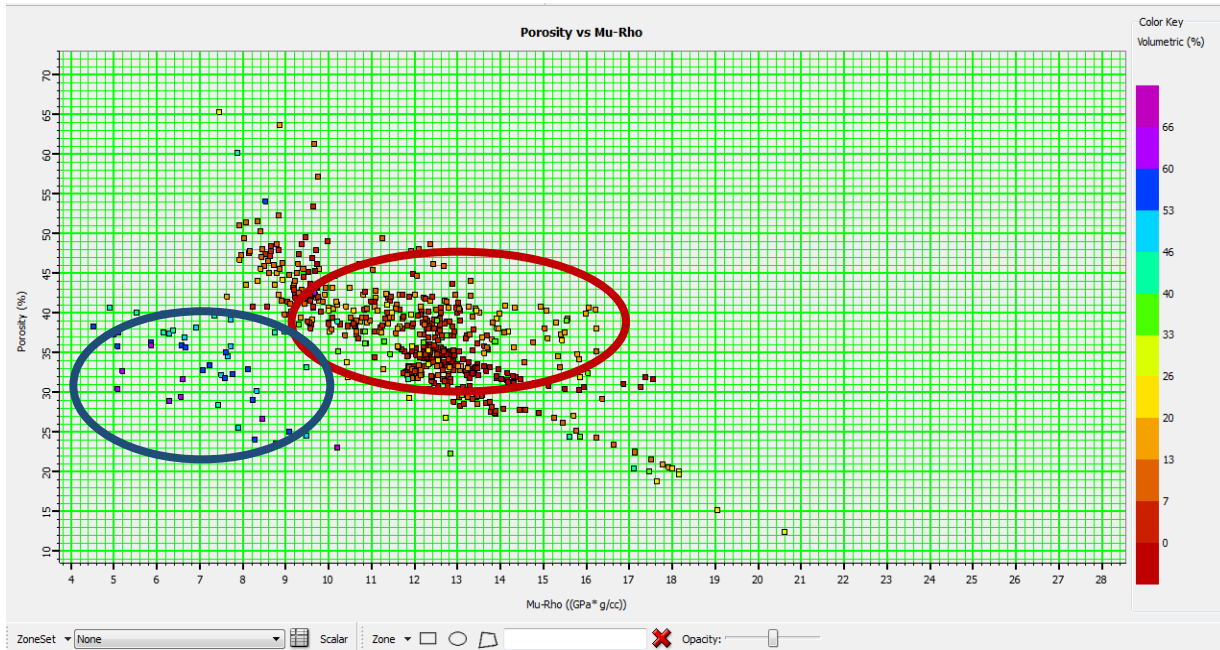


Figure 8b: Cross plot model of Mu-rho versus porosity colour coded with volume of shale for reservoir C10

Inversion Result

The final seismic inversion result (Acoustic impedancemaps) of horizon C10(Figure9)shows similarity in lateral distribution and hydrocarbon prospect zones as seen in the structural time and depth map. . Low acoustic impedance (blue) which indicates sand facies are observed to be close to the drilled wells. Well EK2 is characterized by low acoustic impedance, indicating sand dominating lithology in these zones. Acoustic impedance is a diagnostic seismic attribute that differentiate shale (high acoustic impedance) and sand lithology with low acoustic impedance. Shale lithology is more compacted and have a higher velocity than unconsolidated sand of the Niger Delta hence shale lithology are generally characterized by high acoustic impedance than sand with low value. The Acoustic impedance result complement the structural maps which give credence to further interpretation of delineated hydrocarbon-bearing zones. The regions characterized with low acoustic impedance ($18000\text{g.ft/cm}^3.\text{s}$ - $18600\text{g.ft/cm}^3.\text{s}$) blue colour are indicative of fluid-saturated sand (hydrocarbon). Zones in the South western part of the field with red coloration indicate dominating shale lithology.

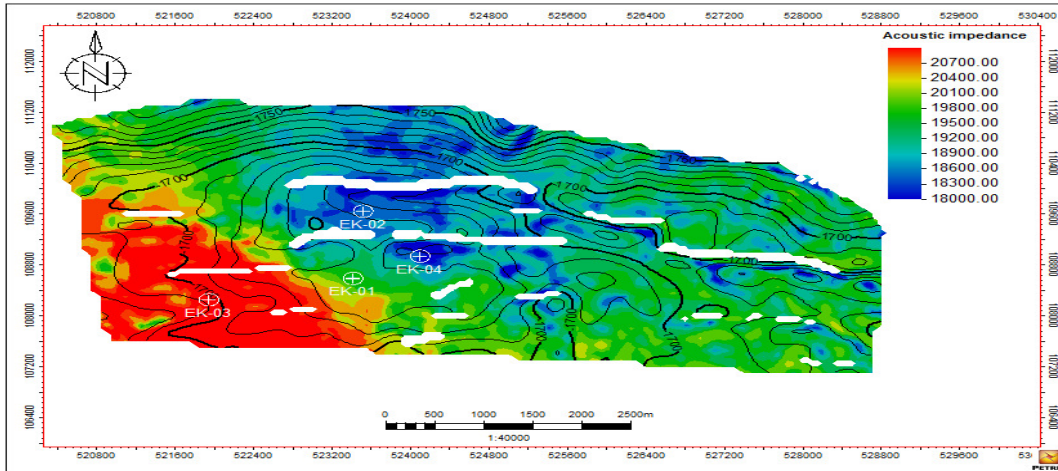


Figure 9: Seismic inversion surface C10

Property Modelling

Petrophysical properties which include porosity and net to gross (NTG) were scaled up into the grid cells using the Arithmetic averaging’ algorithm (Figure 10). The property grids were obtained by populating the geological model developed with well log data. The 3D grid developed include: Porosity and net-to-gross ratio. Upscaled total porosity and NTG were co-kriged with inverted acoustic impedance and were distributed across the grid cells using the sequential gaussian simulation algorithm to build total porosity and NTG models respectively (Figure 11a and 11b).

In (Figure 11a) areas marked light green have the least porosity of about 0.17-0.20, those marked green yellow have about 0.25-0.30 while regions with red colour have porosity value ranging between 0.30 and above. All the sections in reservoir B20 tend to have high porosity though areas with red have the highest while those with light green have the least value. Similarly, the Net-To-Gross (NTG) model as displayed in Figure 11b indicates that areas with red colour have the highest Net-To-Gross (NTG) value and those with purple colour has the least when compared to others.

The Seismic derived porosity for surface C20 indicate variation of porosity through the reservoir interval and shows the porosity increased in the uppermost part of the reservoir reached to 30% and above, due to increasing of clean sand contain corresponding to high *Net-To-Gross* (NTG) and low acoustic impedance



Figure 10: C10 Upscaled Properties

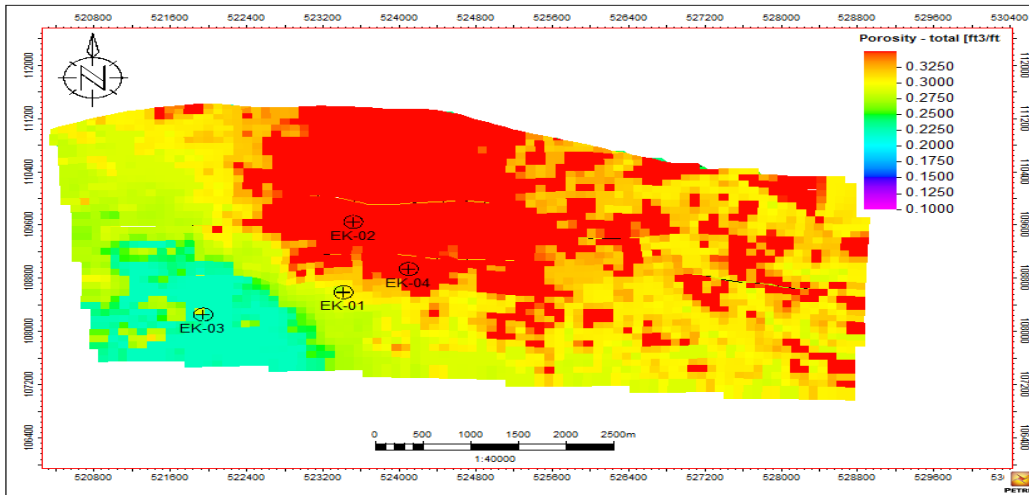


Figure 11a: C10 Total Porosity Property model

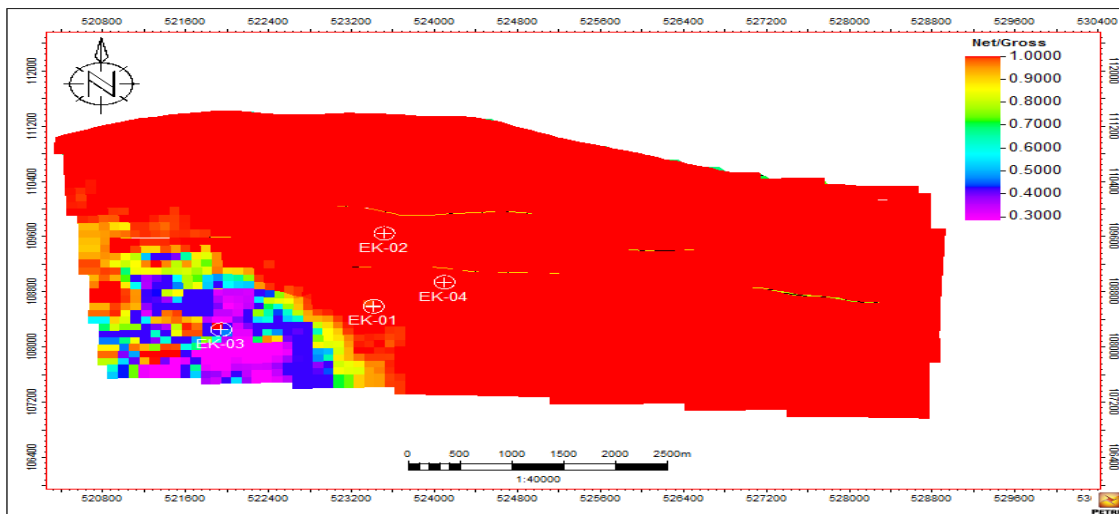


Figure 11b: C10 Net to gross Property model

V. DISCUSSION OF RESULTS

In this study, we have embarked on the delineation and mapping of hydrocarbon-bearing reservoirs from surface seismic sections and well logs within the depth interval of 6065ft (1849m) and 5960ft (1818m).

The petrophysical analysis gave volume of shale with a range of 3.96% to 14.33% indicating high volume of sand which correspond to high net pay zone and clean sands for sand C10. The general average values obtained for total porosity and effective porosity are 25.98% to 31.34% and 24.41% to 32.10%. According to Rider classification [14], porosity measurements < 5% are negligible, between 5-10% are poor, 10-20% are good, 20-30% are very good and > 30 are excellent. Based on this classification scheme which is globally accepted for porosity classification, the total porosity and average effective porosity from reservoir C10 are classed as very good to excellent. The best fit linear relationship in the crossplot of porosity versus P-impedance portray a good correlation coefficient of (0.71) for the reservoir of interest. It is observed that the cross plot model of porosity versus Mu-rho shows that sand is associated with high Mu-rho and porosity corresponding to low volume of shale value while low Mu-rho and

porosity indicate shaly part of the reservoir with high volume of shale. The structural maps (both time and depth map) created demonstrate that the most predominant trap in Field was the growth fault generated rollover anticlines drifting upper east southwest. The rollovers develop as a result of twisting of the downthrown side fault block as it conforms to curve fault surface. The anticlinal trap hydrocarbon may perhaps have gathered at these locally high points in the subsurface, which is where the high contours are closed against fault (Figures. 9a and 9b). The structural maps (both time and depth map) show a possible fluid accumulation that conforms to structure around the wells. The hydrocarbons are transcendently trapped by rollover anticlines and fault closures in Field. The cross plot check the relationship of acoustic impedance with reservoir properties (porosity) which give credence to our interpreted inverted acoustic impedance result and derived porosity section. The inversion results is defined with low acoustic impedance (blue colour, (18000)) around the wells location in the field (Figure 9). The acoustic impedance attribute reveals the most abundant facies in a given area. It shows that most of our sand areas are low acoustic impedance while shaly zones are characterise by high acoustics impedance. Low acoustic impedance areas indicate high porosity area. The porosity map (Figure 11a) shows better porosity around the wells than away from the wells. The porosity value of sandstone porous zone has average range value 25% -32%, which agree with the well logs. The most likely explanation is that porosity in the Niger Delta is a combination of depositional and diagenetic processes, with the diagenetic events destroying primary porosity. Because cleaner sandstones typically have greater original porosity than poorly sorted sandstones, we would expect to see higher predicted porosity in the high depositional-energy channels where percent sand content is higher than outside the channels. The porosity generally decreases with increase clay volume. In the net-to gross ratio that ranges continuously from 0.90 at one end (mostly sand) to 0.04 at the other end (mostly shale.)

VI. CONCLUSION

Integration of well log data and seismic acoustic impedance proved to be an excellent technique to predict reservoir porosity and interpreting seismic data beyond the limitations of well locations. The post-stack inversion for direct prediction of porosity was performed by transformation of acoustic impedance and utilizing an estimated porosity log. The total porosity for depth interval of 6252-6401ft ranging from 25.98% -31.34% in reservoir C10. The acoustic impedance derived porosity has average range value of 25% -32%, which agree with the well logs. The results of the acoustic impedance inversion provides useful means of mitigating the risks associated with the exploratory efforts within the study area. This methodology can also be used for a quick evaluation of other reservoir properties. The results provides an insight about the distribution of useful reservoir properties lithology, porosity, net to gross and hydrocarbon saturation within the area of study.

ACKNOWLEDGMENT

The authors are thankful to World Bank, Africa Centre of Excellence, and University of Port Harcourt and also express their sincere thanks to the SHELL, Nigeria for access to their data.

REFERENCES

- [1] Goodway, B., Chen, T., and Downton, J., Improved AVO Fluid detection and lithology discrimination using Lamé's Petrophysical parameters; " λ/ρ , μ/ρ , γ/μ Fluid stack" P and S inversions, Proceedings of the 67th Annual International Meeting of Society of Exploration Geophysicists held in Dallas, Texas, November (1997) 2-7.
- [2] Çemen, I., Fuchs, J., Coffey, B., Gertson, R., Hager, C., Correlating porosity with acoustic impedance in sandstone gas reservoirs: examples from the Atokan sandstones of the Arkoma Basin, Southeastern Oklahoma. AAPG, Annual Convention Exhibition, Pittsburgh, Pennsylvania (2014). Search and Discovery Article #41255.
- [3] Dolberg, D. M., Helgesen, J., Hanssen, T. H., Magnus, I., Saigal, G., and Pedersen, B. K., Porosity prediction from seismic inversion, Lavrans Field, Halten Terrace, Norway, *The Leading Edge* (2000), **19**(4), 392-399.

- [4] Doyen, P. M., Porosity from seismic data—A geostatistical approach: *Geophysics* (1988), 53, 1263–1275.
- [5] Corredor, F., Shaw, J.H., Bilotti, F. Structural styles in the deepwater fold and Thrust belts of the Niger Delta. *AAPG Bull* (2005). 89 (6), 753–780.
- [6] Short K.C. and Stauble A.J. Outline of the geology of Niger Delta, American Association of Petroleum Geologists Bulletin (1967), 51 p. 761-779.
- [7] Evamy B.D., Haremboure J., Kamerling P., Knaap W.A., Molloy F.A., and Rowlands P.H., Hydrocarbon habitat of Tertiary Niger Delta: American Association of Petroleum Geologists Bulletin (1978), v. 62, p. 1-39.
- [8] Whiteman A. J. Nigeria: Its petroleum geology, resources and potentials(1982). (1) 176, (2) 238. Graham and Trotman, London, U.K.
- [9] Larionov, V. Borehole Radiometry: Moscow, U.S.S.R., Nedra (1969).
- [10] Schlumberger. Log Interpretation Principles, Applications. Houston: Schlumberger Educational Services(1974), pp.1 – 198.
- [11] Dresser, A. Log Interpretation Charts. Dresser Industries Inc., Houston, Texas. (1979): p.107
- [12] Gaymard, R., Poupon, A., Response of neutron and formation density logs in hydrocarbon-bearing formations. SPWLA (1968).
- [13] Archie, G. E.The Electrical Resistivity Log as an aid in de-termining some Reservoir Characteristics. *Journal of Petroleum Technology*. (1942), Vol.5: pp.54-62 <https://doi.org/10.2118/942054-G>.
- [14] Rider, M.H. *The geological interpretation of well logs*. Blackie and sons Ltd., Glasgow and London (1986).